Remote Near-IR Light Activation of a Hyaluronic Acid/Poly(L-lysine) Multilayered Film and Film-Entrapped Microcapsules

D. V. Volodkin,* M. Delcea, H. Möhwald, and A. G. Skirtach*

Max-Planck Institute of Colloids and Interfaces, Research Campus Golm, Potsdam D-14424, Germany

ABSTRACT Spontaneous embedding of gold nanoparticle (NP) aggregates or polyelectrolyte microcapsules modified with NPs in biocompatible hyaluronic acid/poly(L-lysine) films is reported. The NPs were adsorbed in the aggregated state to induce near-IR light absorption. The films functionalized with gold NPs become active in response to a "biologically friendly" near-IR laser at a power of about 20 mW. The activation is characterized by a localized temperature increase in the film, allowing conversion of light energy to heat into confined volumes. Microcapsules adsorbed onto the film can release its cargo under stimulation with near-IR light because of localized permeability changes in their walls. This work is aimed at layer-by-layer film-based biomedical coatings and active surfaces with light-sensitive features wherein metal NPs and microcapsules are used as active centers or carriers with remote control of functionalities.

KEYWORDS: layer-by-layer • multilayered polyelectrolyte film • microcapsule • IR light • remote release • stimuli-sensitive.

INTRODUCTION

Nanoengineered biomaterials are playing an increasing role in biomedicine and drug delivery. Nanotechnology allows the construction of multifunctional and smart systems that satisfy strict requirements in drug delivery. The layer-by-layer (LbL) deposition technique (1) has been widely employed to engineer advanced biomaterials and to develop nanoscale drug release systems (2−7). The method is based on consecutive adsorption of species having the ability to interact with each other such as in the instance of oppositely charged polyelectrolytes. The technique is a powerful instrument that offers the advantage of large flexibility with respect to immobilization methods (8, 9) and allows the incorporation of diverse bioactive constituents, namely, proteins and enzymes (10−12), surface-supported lipid membranes (13), nucleic acids (14−16), liposomes (17−20), and viruses (21). Surface functionalization with bioactive materials utilizing the LbL method can be performed by either active or passive loading (22−26). Biopolymers such as polyanions [hyaluronic acid (HA), poly(glutamic acid), chondroitin sulfate, etc.] and polycations [poly(L-lysine) (PLL), chitosan, etc.] (27−32) used to construct LbL films can provide not only biocompatible/biodegradable characteristics to the films but also high loading capacity. In contrast to linearly growing films characterized by the nanometer thickness per deposited layer, the films prepared using such biopolymers exhibit mostly exponential growth, i.e., that in which the polymer mobility is high and the film thickness reaches a micrometer scale.

Release stimulated from a distance (remote release) is desired to minimize drug toxicity by effective local drug delivery. Light-stimulated remote release is of special interest because of external control of the light intensity and modulation and its noninvasive character, which is desired for bioapplications. In this regard, noble metal nanoparticles (NPs) are attractive candidates to induce local nanometer-scale heating. That can also be used for functionalization of spherical particles such as liposomes and microcapsules (33−35), providing unique and tunable optoelectronic properties. A particularly interesting application of such NPs is remote initiation and manipulation of the intracellular activity (36−38). It was recently demonstrated that NPs can be used as active nanometer-scale heating centers to controllably affect the permeability of the polymeric network (34). When heated above the glass transition temperature, the crystalline polymeric network loosens and softens transiently, permitting the release of encapsulated materials through the membrane (34). The feasibility of such remote control was shown for polymeric microcapsules. With regard to planar films and their functionalization with NPs, most studies conducted to date considered synthetic polymers (39−41). Besides, no external excitation has been studied on the films functionalized with light-sensitive material, metal NPs or microcapsules.

Here we present the results of functionalization of biocompatible HA/PLL films by gold NPs and polymeric microcapsules (42) containing gold NPs. Film functionalization with NPs aims to control the temperature on the LbL coated supports, whereas integration of microcapsules in the film makes it possible to use the films as reservoirs that are able to release their content upon light stimulation. The functionalized films inherit optoelectronic properties of NPs and become active; this function stems from the property of NPs

* Corresponding authors. E-mail: dmitry.volodkin@mpikg.mpg.de (D.V.V.), skirtach@mpikg.mpg.de (A.G.S.). Tel: +49-(0)-331-567-9235. Fax: +49-(0)-331-567-9202.

Received for review April 21, 2009 and accepted June 30, 2009

DOI: 10.1021/am900269c

to absorb electromagnetic energy and convert it to heat. The mechanism relies on surface plasmon resonance absorption and a subsequent temperature rise on the NPs upon exposure to laser light (43, 44). Heat is localized to nanometer-sized areas, and it can be regulated by the incident intensity, size, and aggregation state of the NPs (45). Near-IR absorption is relevant for biomedical applications, and NP aggregates possess the desired absorption in this spectral range (41). Therefore, in this work, films and microcapsules have been modified with NP aggregates. The light-induced activity with regard to external, near-IR laser excitation is studied for both films, functionalized either with NPs or with microcapsules.

EXPERIMENTAL SECTION

Materials. PLL hydrobromide with a viscosimetric molecular mass of 15−30 kDa (ref P7890), PLL labeled with FITC (PLL-FITC; ref P3543, 15−30 kDa), poly(styrenesulfonate) (PSS; ref 24,305-1, 70 kDa), hydrophilic colloidal gold NPs (20 nm), rhodamine−dextran (ref R9379, 70 kDa), and poly(diallyldimethylammonium chloride) (PDADMAC; 200−350 kDa) were purchased from Sigma-Aldrich (Germany). The NP concentration was determined to be 10^{12} NPs/mL. HA with a viscosimetric molecular mass of 360 kDa was purchased from Lifecore Biomedical (Chaska, MN; ref 002570). Throughout this study, 10 mM Tris containing 15 mM NaCl, pH 7.4, was used and will be mentioned in the text as Tris buffer. The water used in all experiments was prepared in a three-stage Millipore Milli-Q Plus 185 purification system and had a resistivity higher than 18.2 MΩ cm.

Preparation of the Films. The polyelectrolyte multilayer films $(PLL/HA)_{24}$/PLL were prepared by the LbL technique using a dipping robot (Riegler & Kirstein GmbH, Berlin, Germany). The films were deposited either onto a microscopy cover glass (12 mm in diameter; Marienfeld GmbH, Lauda-Königshofen, Germany) or on dialysis membranes from regenerated cellulose with cutoff 10 kDa (ref 132118; Spectra/por, Spectrum Labs, Rancho Dominguez, CA). Before deposition, the glass slides were cleaned by consecutive incubation in hot solutions (60 °C) of 2% (w/v) Hellmanex (Hellma GmbH, Müllheim, Germany), 0.01 M sodium dodecyl sulfate, and 0.1 M HCl for 15 min each solution followed by multiple rinsing with pure water. The membrane was used without any additional cleaning. The film buildup was pursued at 25 °C by alternating dipping of the glass slides into PLL (0.5 mg/mL) and HA (0.5 mg/mL) solutions in a Tris buffer with an intermediate washing step with the buffer for 10 min. Before deposition, polyelectrolyte solutions were filtered through a 0.45 μm filter. Each dipping step lasted over 10 min. The abbreviation $(PLL/HA)_x$ is given to the film prepared by $2x$ alternating polyelectrolyte adsorption steps (layers) or x pairs of bilayers. In the case of cover glasses, the number of layers has been chosen as $(PLL/HA)_{24}$/PLL for the films made on the membrane $(PLL/HA)_{48}$/PLL. In order to prepare the film labeled with FITC, PLL-FITC was added to the PLL solution used for film deposition at a weight ratio of unlabeled PLL to labeled PLL of 30:1.

In order to quantify the amount of PLL released from the film and in contact with the NP suspension (200 μL) for 15 min, the film prepared with PLL-FITC was removed from the glass substrate by the addition of 200 μL of 0.05 M NaOH followed by a 5 min incubation in this solution. This treatment allows for the complete removal of the multilayer film by deprotonation of PLL molecules. Then 1.35 mL of a Tris buffer was added. The fluorescence intensity was then measured with a fluorometer (Fluoromax-4, Horiba Jobin Yvon, Edison, NJ). The excitation wavelength was set at 490 nm, and the emission was measured at 520 nm. The amount of PLL in the film has been measured using a calibration curve for the PLL solution with PLL-FITC.

Adsorption of NPs and Microcapsules. Citrate-stabilized colloidal gold NPs were used in the experiments. A total of 0.8 mL of the NP solution was added into a well hosting the freshly prepared $(HA/PLL)_{24}$/PLL film at the bottom. Aggregated NPs were obtained by directly adding gold NPs into the well with a thick gel film possessing the last layer PLL, followed by incubation for 1 h at room temperature. The films were washed for 5 min with water before the solution with the NPs was added. UV−vis absorption spectra of both the films and supernatants were measured.

Polyelectrolyte microcapsules $(PDADMAC/NP/PSS)_4$ containing gold NPs were prepared according to the method described elsewhere with some modifications (44). The capsules were made using the LbL deposition technique and 4.78 μm SiO_2 particles (Microparticles GmbH, Berlin, Germany) as sacrificial cores. Polyelectrolytes were dissolved in 0.5 M NaCl at a concentration of 0.5 mg/mL. SiO_2 templates with PDADMAC as the outermost layer were resuspended in a gold NP suspension (5×10^{11} NPs/mL), which was left before to incubate for half a minute in 0.1 M NaCl. After polyelectrolyte and NP deposition, coated SiO_2 particles were further dissolved in a HF (0.3 M) solution, and the sample was then washed with water until the pH of the solution reached 5. The encapsulation of rhodamine−dextran was done by heating a mixture of capsules in a 0.1 mg/mL rhodamine−dextran/water solution for 20 min at 54 °C. leading to capsule shrinkage to a diameter of about 2 μm. The samples were allowed to cool for 5 min and washed twice with water to remove nonencapsulated rhodamine−dextran. Further the microcapsules were adsorbed on the $(HA/PLL)_{24}$/PLL film by the addition of 50 μL of the capsule suspension (2×10^6 capsules/mL in a Tris buffer) on the top of the glass coverslip coated with the freshly prepared film. After 1 h of incubation, the film was intensively washed three times with a Tris buffer.

Atomic Force Microscopy (AFM) Characterization. The measurements were conducted on a dried film in the tapping mode by a Veeco (MultiMode) AFM device.

Transmission Electron Microscopy (TEM) Characterization. For these measurements, the films were deposited onto a cellulose membrane as described above. The measurements were performed to determine the location of NPs by cutting through the film. The film was first treated with a uranyl acetate solution for increasing the contrast and then placed into a capsule filled with solidifying gel. Then the capsule containing the film was cut through for TEM imaging.

Confocal Laser-Scanning Fluorescence Microscopy (CLSM). CLSM micrographs were taken with a Leica confocal scanning system mounted to a Leica Aristoplan and equipped with a 100× oil immersion objective with a numerical aperture of 1.4. The excitation wavelength was 488 nm for FITC-labeled compounds and 552 nm for rhodamine-labeled ones.

Remote Activation. These experiments were conducted according to the previously described procedures employed for remote release of encapsulated materials. Briefly, the films were marked by a black marker and the images were recorded in a confocal scanning microscope. Then, the holder with the films was positioned in the setup, and the same site was identified by the markers. Subsequently, the film was exposed to a near-IR laser operating at 830 nm. After this step, the holder with the film was placed back into the confocal microscope, and another confocal laser scanning microscope image was taken at the same site.

RESULTS AND DISCUSSION

Figure 1a demonstrates the schematics of a $(HA/PLL)_{24}$/PLL/NP film with gold NPs adsorbed onto its surface. Al-

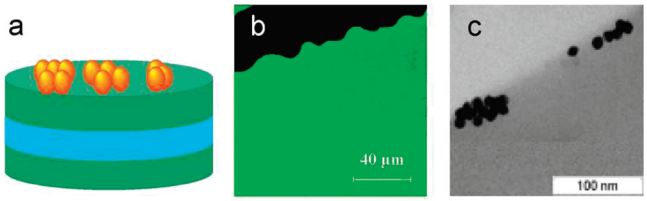

FIGURE 1. (a) Schematic presentation of gold NPs adsorbed onto the surface of a $(PLL/HA)_{24}/PLL$ film. Layers in the film show that the film was made by consecutive polymer deposition; however, the film is in a dynamic state, and the structure is mixed. (b) Confocal microscope image of the film $(PLL/HA)_{24}/PLL/NP$ prepared with PLL-FITC. (c) TEM image of a cross section of the $(PLL/HA)_{48}$ film with adsorbed NPs. The scale bars in parts b and c are 40 and 15 μm, respectively.

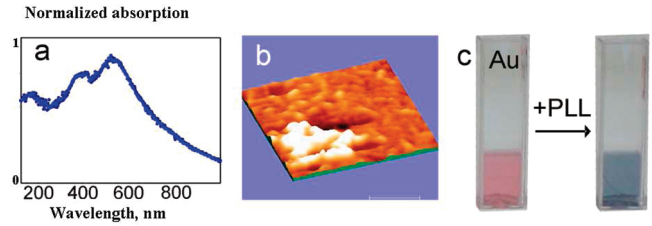

FIGURE 2. (a) Absorption spectrum of the $(PLL/HA)_{24}/PLL/NP$ film with aggregated 20 nm gold NPs. (b) AFM image of the surface of a dried $(PLL/HA)_{24}/PLL/NP$ film showing aggregates of NPs. The *Y* axis is 200 nm. (c) Photographs of cuvettes with gold NP suspensions before and after the addition of a PLL solution.

though the films are present in a dynamic equilibrium state or a mixed configuration (46), they are depicted by layers, reflecting the fact that they were built by the LbL technique. In this regard, linearly growing films such as those composed from PSS, poly(allylamine hydrochloride), and PDADMAC are much thinner. They typically have a few nanometers increase per deposition step and are characterized by strong interpolymer interaction and low polymer mobility in the films. At the same time, the growth regime can be triggered by film preparation conditions (47) and the addition of other polyelectrolytes or LbL deposition of another polymer pair (48, 49). For instance, films growing linearly at room temperature can switch to exponential growth at higher temperature because of faster polymer diffusion (47). The principal difference of exponentially growing films from linearly growing LbL counterparts is that their thickness is in the micrometer range because of polymer diffusion "in" and "out" (27, 28, 46, 48, 50). Therefore, CLSM can be used to investigate their structure. The surface scan of the FITC-labeled films (Figure 1b) shows uniformity in their structure. The black area is a scratch made in the film to enhance the contrast of the image. Although optical microscopy reveals the general features and can be used for fast, routine characterization of the aggregates, their detailed configuration can be observed by electron microscopy. A slice of the TEM image through the film demonstrates that gold NPs are located only at the surface, presumably because of diffusion limitations through the whole film (Figure 1c). Srivastava et al. (51) reported the strong accumulation of 4 nm quantum dots in the exponentially growing PDADMAC/poly(acrylic acid) films, which can spontaneously diffuse within the film but also partly diffuse out from the film with time, indicating no significant diffusion problems. We suppose that, because of their large size, 20 nm gold NPs do not diffuse into the HA/PLL film. The same is the case for larger microcapsules. In the case of films to be imaged with CLSM, the number of layers has been chosen as $(PLL/HA)_{24}/PLL$ and for the films made on the cellulose membrane as $(PLL/HA)_{48}/PLL$. The higher number of layers in the latter case is due to the inhomogeneous structure of the film formed on the membrane. This can be explained by the lower affinity of the polyelectrolytes to the cellulose surface than to glass.

The absorption spectrum of a NP-modified film is presented in Figure 2a. The peaks of both the surface plasmon resonance absorption of gold NPs, 520 nm, and the aggregates of gold NPs, ~620 nm, can be seen here. Similar positions of the peaks were registered for the NP suspension in contact with the film. AFM can be used to gain insight into the aggregates (Figure 2b). One can see NP aggregates on the surface of a dried film. Aggregates of micrometer sizes (typically from 1 to 5 μm) have been registered on the wet film surface by optical microscopy (data not shown). The aggregates observed by AFM are much smaller; they are in the minority but should have the same structure as larger ones because the larger aggregates are grown from smaller ones. The amount of loaded NPs is relatively high. A loading capacitiy of around 100 $\mu g/cm^2$ has been determined for $(PLL/HA)_{24}/PLL$, which can adsorb all of the NPs from solution in 2 days of incubation.

The structures of HA/PLL films have been thoroughly studied, and their exponential growth regime is attributed to PLL diffusion into the whole film (27, 28, 46). Jourdainne et al. showed that in the film with 24 bilayers PLL is present in two populations: mobile and immobile (46), with diffusion coefficients on the order of 10^{-1} (or higher) and below 10^{-3} $\mu m^2/s$ for mobile and immobile components, respectively. The mechanism of film formation has been described by so-called polymer diffusion "in" and "out" and by alternative/complementary theory involving two main zones in the film structure: "diffusion" and "restructuration" zones, where PLL migration within the film is pronounced or restricted, respectively (31). The exponentially grown HA/PLL films made in this study are considered to be in dynamic equilibrium, and, therefore, adsorption conditions are expected to be different from those for typical polyelectrolyte multilayer thin films assembled in the linearly growing regime, whose characteristic feature is restricted mobility of the polymers.

It was found in our studies that the dynamical equilibrium affects both adsorption and the aggregated state of NPs. The LbL films studied here were terminated with a positively charged PLL layer for increased interaction with negatively charged citrate NPs used in this work. NPs are found to aggregate immediately upon addition to the $(HA/PLL)_{24}/PLL$ films. The aggregation can be clearly observed because the solution changes color from pink to blue. It is known that salt induces aggregation of the citrate-stabilized NPs used in this work (33), and the films fabricated in a Tris buffer with 15 mM NaCl can contain substantial amounts of salt ions. Therefore, to remove free salt ions, the films were washed with water before the solution with NPs is added.

To find if salt ions bound to the polyelectrolytes in the film (not removed after water washing) are responsible for aggregation, we have performed the following experiments. Salt was added to the film, which had already been covered with NPs. For this purpose, we have removed the supernatant solution with previously adsorbing NPs and added a Tris buffer to the film followed by 15 min of incubation to dope the salt into the film. After water washing, a fresh batch of gold NPs was added to the film. No NP aggregation in the supernatant was observed in this case, and no further NP adsorption has been registered. If the same procedure was conducted with PLL instead of salt, NP aggregation was observed again. These experiments demonstrate that PLL molecules but not salt ions are responsible for NP aggregation in supernatants and NP adsorption on the film. We assume that high PLL mobility in the film promotes fast release of the PLL molecules to the film surface in order to make additional contacts with adsorbing NPs. Moreover, PLL can diffuse from the film to the bulk solution, which contains NPs. This process can be driven by the formation of a PLL/NP complex in the supernatant, which subsequently leads to adsorption of NP aggregates onto the film.

To further confirm these data and find the threshold concentration that induces the aggregation, we mixed PLL polymers at various concentrations with the solution of NPs. Both visual and UV−vis absorption was used for characterization. It was found that the presence of 2.5×10^{-5} mg/mL PLL in the NP suspension does not lead to aggregation, but 2.5×10^{-4} mg/mL induces visible NP aggregation, as shown in Figure 2c. Thus, the concentration of the PLL polymers needed to induce NP aggregation is in the range of $(0.25-2.5) \times 10^{-4}$ mg/mL, and this corresponds to a PLL/NP number ratio of 0.5−5, respectively. This shows that a low concentration of PLL (NPs are present in 2 times excess than PLL molecules) is not enough to assemble the NPs. The PLL concentration in the NP suspension added to the film (15 min incubation) was found to be 1.1×10^{-4} mg/mL, which is in the range of the PLL concentration needed to induce NP aggregation. A control experiment showed that the filtered NP suspension does not induce PLL release from the film. Thus, PLL release from the film is attributed to film interaction with NPs, as suggested above. It should be noted that HA does not induce aggregation even at higher concentrations than in the case of PLL, showing that the NP−polymer interaction is of electrostatic origin.

As described above, NP aggregates induce absorption in the biologically "friendly" near-IR spectral range because of dipole−dipole interaction on neighboring NPs. We use this property for remote activation of the films by a laser operating at 830 nm. As was mentioned earlier, inherent parameters that influence the activation are the NP size and their concentration. Other parameters that can be adjusted are the aggregation state of NPs and incident intensity. For the largest aggregates attained in this work, the activation of the films was observed at intensities above 20 mW of the laser focused through a 100× objective onto the film in the area of one squared micrometer. Figure 3a shows a transmission

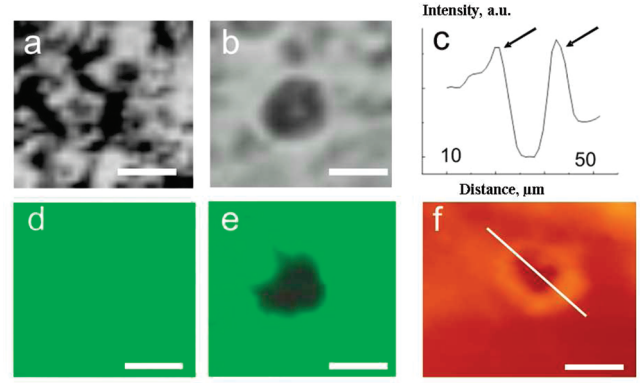

FIGURE 3. Creation of incisions at the film surface: morphology of the $(PLL/HA)_{24}$/PLL/NP film before illumination by a laser light in transmission and fluorescence modes, parts a and d, respectively. The film after illumination by a laser light with 50 mW of incident power in transmission and fluorescence modes, parts b and e, respectively. An AFM profile (c) was taken for the same area but with a dried sample through a line in the image (f). Black arrows in graph c show the position of the rim of the effected area. The scale bar corresponds to 10 μm.

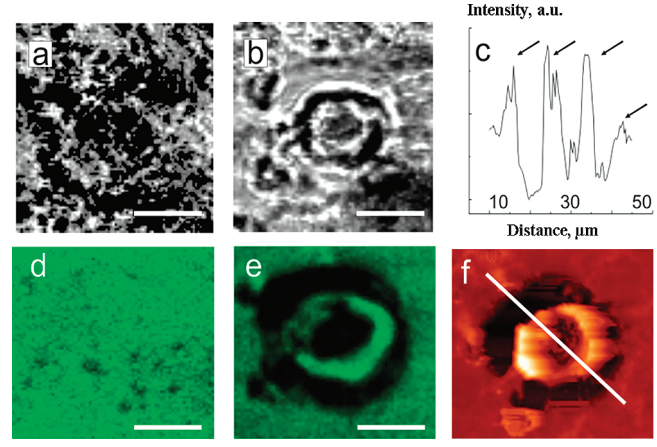

FIGURE 4. Creation of incisions at the film surface: morphology of the $(PLL/HA)_{24}$/PLL/NP film before illumination by a laser light in transmission and fluorescence modes, parts a and d, respectively. The film after illumination by a laser light with 80 mW of incident power in transmission and fluorescence modes, parts b and e, respectively. An AFM profile (c) was taken for the same area but with a dried sample through a line in the image (f). Black arrows in graph c show the position of the rim of the effected area. The scale bar corresponds to 10 μm.

confocal scanning microscopy image of the film with aggregates of gold NPs (dark areas). The corresponding CLSM fluorescence image shows high fluorescence before laser illumination (Figure 3d). In the remote activation, the film with aggregates of gold NPs was illuminated by laser light with power of 50−80 mW, resulting in a change of the film's morphology and the creation of localized incisions or the destruction of the film surface, as shown in Figure 3b. The decreased fluorescence in Figure 3e is the result of the local heating effect on the film.

Figure 4 presents the results obtained after illumination of the films with higher intensities. Specifically, at incident intensities above 80 mW, sufficiently large (on the order of micrometers) aggregates of gold NPs caused local "explosion", leading to the destruction of the film (Figure 4e,f). A characteristic feature of locally activated films is the presence

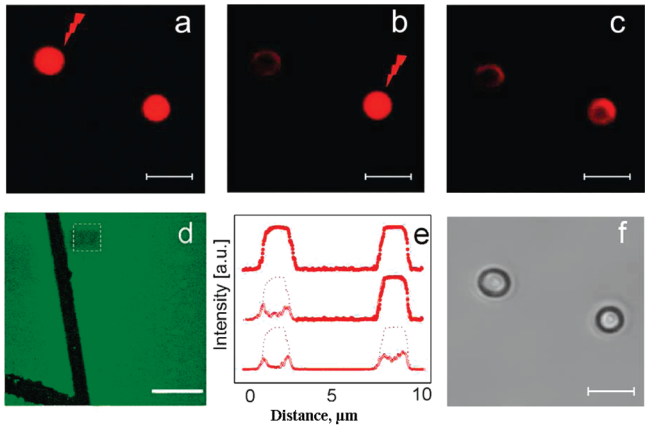

FIGURE 5. Adsorption of microcapsules onto the $(PLL/HA)_{24}$/PLL films. (a–c) CLSM images of the capsules exposed to the near-IR light irradiation. (d) CLSM image of the film surface (the film is prepared with PLL-FITC; black lines are scratches made by a needle for easier film imaging). (e) Cross-sectional profile of the capsules after step-by-step laser exposure (the sections from top to bottom correspond to the images a–c, respectively). The scale bar in parts a–c and f is 4 μm. (f) TEM images of the capsules after light irradiation. The scale bar in part d is 25 μm.

of a rim, denoted by arrows in Figures 3c and 4c, around the increased temperature area. Such a rim was also observed for NPs embedded in a polymeric film (52).

Defocusing or reduction of the laser intensity led to no visible morphological changes. The origin of the observed near-IR laser activation of the films is the local disruption of the polymer network due to a high local temperature increase. The polymers get pushed out of the film, while the film is stabilized because of thermal cross-linking of the polymers. The thermal cross-linking between the amino groups of PLL and the carboxylic groups of HA is expected to take place because of high local temperature. Covalent thermal cross-linking between the above-mentioned chemical groups leads to the formation of covalent amide bonds at temperatures of 130–150 °C (53, 54). It can be noted that such heating is localized to nanometer-sized areas, and that makes such operations nondestructive on the macroscale.

Microcapsules can also be adsorbed on the hydrogel HA/PLL film by direct contact of the film and the capsules. The opposite charges in polyelectrolyte multilayers of microcapsules are almost compensated for overall (55), but microcapsules' strong attachment to the film (no capsule removal observed upon intensive film washing) can be attributed to some uncompensated negative charges on the last layer. We believe that the immersed capsules adapt to the "best" position in terms of interaction with the PLL molecules, which can be doped from the whole film to the film surface because of high mobility (46). Immobilization of macromolecules and stiff particles in the HA/PLL film is a topic of our separate study (56). The microcapsules filled with rhodamine–dextran were premodified with gold NPs and were successfully embedded in the film. Figure 5a presents two capsules on the film surface, while the surface scan of the FITC-labeled $(PLL/HA)_{24}$/PLL film with adsorbed microcapsules on top shows uniformity of their structure (Figure 5d). The white square in Figure 5d shows the location of two microcapsules used in these experiments. Fluorescence intensity profiles of microcapsules filled with rhodamine–dextran shown in Figure 5a–c are present in Figure 5e. The top cross-sectional profile corresponds to capsules from Figure 5a. This shows that before exposure to laser light both capsules have a uniform distribution of fluorescent intensity inside. The middle cross-sectional profile corresponds to capsules from Figure 5b and indicates that the microcapsule exposed to IR light (upper left corner) released its contents (rhodamine–dextran), while the second capsule (lower right corner) was not irradiated and presents a uniform distribution of fluorescence intensity inside. In the next step, the second unexposed microcapsule was subjected to the laser beam; it then also released the dextran molecules (Figure 5c). Figure 5f presents the TEM image of these capsules, demonstrating that the capsules keep spherical shape after light irradiation. Destruction of the HA/PLL film functionalized with gold NPs occurs at irradiation with light power over 20 mW, but the microcapsules modified with the NPs keep the integrity at the same conditions but just become more permeable (dextran release is observed as described above). We believe that this can be explained by a more dense and strong capsule shell made from PDADMAC and PSS followed by thermal treatment. After thermal treatment, the capsule shrinks from 4.5 to around 2 μm and the wall becomes thicker and denser (44, 55). The film made from HA/PLL is very soft and probably less stable to local heating around NPs, which takes place upon light absorption. We note that in the near-IR spectral region the films can be activated by nanorods similar to that performed on microcapsules (57). In the near future, we plan to study the effect of NP surface functionalization on mechanical properties of the exponentially growing LbL films. Techniques allowing one to study the surface mechanical properties are well established (58), and gold NPs have been shown to have a strong effect on the mechanical properties of free-standing capsules (59).

In conclusion, we have demonstrated stable adsorption of gold NP aggregates and microcapsules onto biocompatible HA/PLL films. Laser activation of the films can be performed for affecting, releasing, or removing the upper coatings of the films depending on the laser power. Laser activation of the film-supported capsules showed a remote release of encapsulated dextran. Future applications of the work presented here—biocompatible NP/polymeric composite films with remote-release capabilities—are expected in a variety of biomedical applications such as implant biocoatings, tissue engineering, and even antibacterial cleaning (60).

Acknowledgment. We thank A. Heilig for AFM measurements and R. Pitschke for TEM measurements. The support from a Marie-Curie fellowship (EU6 project BIOCOATING) is acknowledged by D.V.V. The PICT-2006-01365 (Max-Planck Society-Argentine SeCyt) grant is kindly acknowledged.

REFERENCES AND NOTES

(1) Decher, G. *Science* **1997**, *277*, 1232.
(2) Tang, Z.; Wang, Y.; Podsiadlo, P.; Kotov, N. A. *Adv. Mater.* **2006**, *18*, 3203.
(3) Ai, H.; Jones, S. A.; Lvov, Y. M. *Cell Biochem. Biophys.* **2003**, *39*, 23.

(4) Ariga, K.; Hill, J. P.; Ji, G. *Macromol. Biosci.* **2008**, *8*, 981.
(5) Volodkin, D. V.; Mohwald, H. Polyelectrolyte Multilayers for Drug Delivery. In *Encyclopedia of Surface and Colloid Science*; Taylor & Francis Group LLC: Boca Raton, FL, 2009; in press.
(6) Skirtach, A. G.; Kreft, O. In *Nanotechnology in Drug Delivery*; de Villiers, M. M., Aramwit, P., Kwon, G. S., Eds.; Springer: Berlin, 2009; DOI: 10.1007/978-0-387-77667-5.
(7) Caruso, F.; Niikura, K.; Furlong, D. N.; Okahata, Y. *Langmuir* **1997**, *13*, 3427.
(8) Ariga, K.; Hill, J. P.; Li, Q. *Phys. Chem. Chem. Phys.* **2007**, *9*, 2319.
(9) Decher, G.; Schlenoff, J. B. *Multilayer Thin Films: Sequential Assembly of Nanocomposite Materials*; Decher, G., Schlenoff, J. B., Eds.; Wiley-VCH: Weinheim, Germany, 2003.
(10) Jessel, N.; Atalar, F.; Lavalle, P.; Mutterer, J.; Decher, G.; Schaaf, P.; Voegel, J.-C.; Ogier, J. *Adv. Mater.* **2003**, *15*, 692.
(11) Ladam, G.; Schaaf, P.; Cuisinier, F. J.; Decher, G.; Voegel, J.-C. *Langmuir* **2001**, *17*, 878.
(12) Lvov, Y.; Ariga, K.; Ichinose, I.; Kunitake, T. *J. Am. Chem. Soc.* **1995**, *117*, 6117.
(13) Wilson, J. T.; Cui, W.; Sun, X. L.; Tucker-Burden, C.; Weber, C. J.; Chaikof, E. L. *Biomaterials* **2007**, *28*, 609.
(14) Lvov, Y.; Decher, G.; Sukhorukov, G. B. *Macromolecules* **1993**, *26*, 5396.
(15) Pei, R.; Cui, X.; Yang, X.; Wang, E. *Biomacromolecules* **2001**, *2*, 463.
(16) Jewell, C. M.; Zhang, J.; Fredin, N. J.; Lynn, D. M. *J. Controlled Release* **2005**, *106*, 214.
(17) Michel, M.; Vautier, D.; Voegel, J.-C.; Schaaf, P.; Ball, V. *Langmuir* **2004**, *20*, 4835.
(18) Volodkin, D.; Schaaf, P.; Mohwald, H.; Voegel, J.-C.; Ball, V. *Soft Matter* **2009**, *5*, 1394.
(19) Volodkin, D. V.; Arntz, Y.; Schaaf, P.; Möhwald, H.; Voegel, J.-C.; Ball, V. *Soft Matter* **2008**, *4*, 122.
(20) Volodkin, D. V.; Michel, M.; Schaaf, P.; Voegel, J.-C.; Mohwald, H.; Ball, V. Liposome Embedding into Polyelectrolyte Multilayers: A New Way to Create Drug Reservoirs at Solid-Liquid Interfaces. *Advances in Planar Lipid Bilayers and Liposomes*; Elsevier: Amsterdam, The Netherlands, 2008.
(21) Dimitrova, M.; Arntz, Y.; Lavalle, P.; Meyer, F.; Wolf, M.; Schuster, C.; Haïkel, Y.; Voegel, J.-C.; Ogier, J. *Adv. Funct. Mater.* **2007**, *17*, 233.
(22) Jessel, N.; Oulad-Abdelghani, M.; Meyer, F.; Lavalle, P.; Haikel, Y.; Schaaf, P.; Voegel, J.-C. *Proc. Natl. Acad. Sci. U.S.A.* **2006**, *103*, 8618.
(23) Schneider, A.; Vodouhê, C.; Richert, L.; Francius, G.; Le Guen, E.; Schaaf, P.; Voegel, J.-C.; Frisch, B.; Picart, C. *Biomacromolecules* **2007**, *8*, 139.
(24) Vodouhê, C.; Le Guen, E.; Mendez Garza, J.; Francius, G.; Déjugnat, C.; Ogier, J.; Schaaf, P.; Voegel, J.-C.; Lavalle, P. *Biomaterials* **2006**, *27*, 4149.
(25) Volodkin, D. V.; Petrov, A. I.; Prevot, M.; Sukhorukov, G. B. *Langmuir* **2004**, *20*, 3398.
(26) Srivastava, S.; Ball, V.; Podsiadlo, P.; Lee, J.; Ho, P.; Kotov, N. A. *J. Am. Chem. Soc.* **2008**, *130*, 3748.
(27) Lavalle, P. P.; Picart, C.; Cuisinier, F. J. G.; Decher, G.; Schaaf, P.; Voegel, J. C. *Biophys. J.* **2002**, *82*, 53a.
(28) Picart, C.; Lavalle, P.; Hubert, P.; Cuisinier, F. J. G.; Decher, G.; Schaaf, P.; Voegel, J. C. *Langmuir* **2001**, *17*, 7414.
(29) Picart, C.; Mutterer, J.; Richert, L.; Luo, Y.; Prestwich, G. D.; Schaaf, P.; Voegel, J. C.; Lavalle, P. *Proc. Natl. Acad. Sci. U.S.A.* **2002**, *99*, 12531.
(30) Laugel, N.; Betscha, C.; Winterhalter, M.; Voegel, J.-C.; Schaaf, P.; Ball, V. *J. Phys. Chem. B* **2006**, *110*, 19443.
(31) Porcel, C.; Lavalle, P.; Decher, G.; Senger, B.; Voegel, J.-C.; Schaaf, P. *Langmuir* **2007**, *23*, 1898.
(32) Salomäki, M.; Vinokurov, I. A.; Kankare, J. *Langmuir* **2005**, *21*, 11232.
(33) Volodkin, D. V.; Skirtach, A. G.; Mohwald, H. *Angew. Chem., Int. Ed.* **2009**, *48*, 1807.
(34) Skirtach, A. G.; Karageorgiev, P.; Bedard, M. F.; Sukhorukov, G. B.; Mohwald, H. *J. Am. Chem. Soc.* **2008**, *130*, 11572.
(35) Wu, G. H.; Milkhailovsky, A.; Khant, H. A.; Fu, C.; Chiu, W.; Zasadzinski, J. A. *J. Am. Chem. Soc.* **2008**, *130*, 8175.
(36) De Koker, S.; De Geest, B. G.; Cuvelier, C.; Ferdinande, L.; Deckers, W.; Hennink, W. E.; De Smedt, S.; Mertens, N. *Adv. Funct. Mater.* **2007**, *17*, 3754.
(37) Javier, A. M.; del Pino, P.; Bedard, M. F.; Ho, D.; Skirtach, A. G.; Sukhorukov, G. B.; Plank, C.; Parak, W. J. *Langmuir* **2008**, *24*, 12517.
(38) Skirtach, A. G.; Javier, A. M.; Kreft, O.; Kohler, K.; Alberola, A. P.; Mohwald, H.; Parak, W. J.; Sukhorukov, G. B. *Angew. Chem., Int. Ed.* **2006**, *45*, 4612.
(39) Kozlovskaya, V.; Kharlampieva, E.; Khanal, B. P.; Manna, P.; Zubarev, E. R.; Tsukruk, V. V. *Chem. Mater.* **2008**, *20*, 7474.
(40) Tokarev, I.; Minko, S. *Soft Matter* **2009**, *5*, 511.
(41) Lu, C.; Mohwald, H.; Fery, A. *J. Phys. Chem. C* **2007**, *111*, 10082.
(42) De Geest, B. G.; De Koker, S.; Sukhorukov, G. B.; Kreft, O.; Parak, W. J.; Skirtach, A. G.; Demeester, J.; De Smedt, S. C.; Hennink, W. E. *Soft Matter* **2009**, *5*, 282.
(43) Ghosh, P.; Han, G.; De, M.; Kim, C. K.; Rotello, V. M. *Adv. Drug Delivery Rev.* **2008**, *60*, 1307.
(44) Bedard, M. F.; Braun, D.; Sukhorukov, G. B.; Skirtach, A. G. *ACS Nano* **2008**, *2*, 1807.
(45) Skirtach, A. G.; Dejugnat, C.; Braun, D.; Susha, A. S.; Rogach, A. L.; Parak, W. J.; Mohwald, H.; Sukhorukov, G. B. *Nano Lett.* **2005**, *5*, 1371.
(46) Jourdainne, L.; Lecuyer, S.; Arntz, Y.; Picart, C.; Schaaf, P.; Senger, B.; Voegel, J. C.; Lavalle, P.; Charitat, T. *Langmuir* **2008**, *24*, 7842.
(47) Salomaki, M.; Vinokurov, I. A.; Kankare, J. *Langmuir* **2005**, *21*, 11232.
(48) Porcel, C.; Lavalle, P.; Ball, V.; Decher, G.; Senger, B.; Voegel, J.-C.; Schaaf, P. *Langmuir* **2006**, *22*, 4376.
(49) Salomaïki, M.; Kankare, J. *Biomacromolecules* **2009**, *10*, 294.
(50) Boulmedais, F.; Ball, V.; Schwinte, P.; Frisch, B.; Schaaf, P.; Voegel, J. C. *Langmuir* **2003**, *19*, 440.
(51) Srivastava, S.; Ball, V.; Podsiadlo, P.; Lee, J.; Ho, P.; Kotov, N. A. *J. Am. Chem. Soc.* **2008**, *130*, 3748.
(52) Skirtach, A. G.; Mohwald, H. *Appl. Phys. Lett.* **2009**, in press.
(53) Harris, J. J.; DeRose, P. M.; Bruening, M. L. *J. Am. Chem. Soc.* **1999**, *121*, 1978.
(54) Lee, S. W.; Kim, B.-S.; Chen, S.; Shao-Horn, Y.; Hammond, P. T. *J. Am. Chem. Soc.* **2009**, *131*, 671.
(55) Kohler, K.; Mohwald, H.; Sukhorukov, G. B. *J. Phys. Chem. B* **2006**, *110*, 24002.
(56) Volodkin, D.; Madaboosi, N.; Blacklock, J.; Skirtach, A. G.; Mohwald, H. *Langmuir* **2009**, submitted for publication.
(57) Skirtach, A. G.; Karageorgiev, P.; De Geest, B. G.; Pazos-Perez, N.; Braun, D.; Sukhorukov, G. B. *Adv. Mater.* **2008**, *20*, 506.
(58) Fery, A.; Weinkamer, R. *Polymer* **2007**, *48*, 7221.
(59) Bedard, M. F.; Munoz-Javier, A.; Mueller, R.; del Pino, P.; Fery, A.; Parak, W. J.; Skirtach, A. G.; Sukhorukov, G. B. *Soft Matter* **2009**, *5*, 148.
(60) Corbitt, T. S.; Sommer, J. R.; Chemburu, S.; Ogawa, K.; Ista, L. K.; Lopez, G. P.; Whitten, D. G.; Schanze, K. S. *ACS Appl. Mater. Interfaces* **2009**, *1*, 48.

AM900269C